PHYSICAL REVIEW C VOLUME 23, NUMBER 6 JUNE 1981

# Radiative capture of in-flight pions by $^{15}N$

G. W. Reynaud and F. Tabakin
*Department of Physics and Astronomy, University of Pittsburgh, Pittsburgh, Pennsylvania 15260*
(Received 1 December 1980)

In-flight radiative capture cross sections have been studied for the process $^{15}N(\pi^+,\gamma)^{15}O$(g.s.). Total and differential cross sections have been calculated, and the effects of pion distortions, of higher order photoproduction operators, and of nuclear structure have been examined. The Blomqvist-Laget photoproduction operator has been used in an appropriately time-reversed form, the Stricker, McManus, and Carr pion optical potential has been used to account for pion distortions, and the nuclear structure information has been stipulated by use of simple shell model wave functions or by fitting recent electron scattering form factors. Particularly interesting interference effects due to the pion propagator and enhanced isobar contributions are revealed by this study.

[NUCLEAR REACTIONS $^{15}N(\pi^+,\gamma)^{15}O$(g.s.); in-flight capture 50 MeV pions; distorted waves; shell model wave functions; fit to $M1$ form factor; total and differential cross sections.]

## I. INTRODUCTION

Radiative pion capture to discrete nuclear states is a difficult experiment, because essentially all of the pion energy is converted into the energy of the photon, and high energy photons are difficult to resolve. However, in the case of $^{15}N(\pi^+,\gamma)^{15}O$ the experiment is feasible because of the large energy separation between the ground and first excited states of $^{15}O$(~5 MeV). We show in this work that the dependence of the total and differential cross sections on the various terms in the radiative capture transition operator, on the nuclear structure, and on the initial pion distorted waves yields some interesting and surprising insights into the dynamics of the $^{15}N(\pi^+,\gamma)^{15}O$ (g.s.) reaction. These insights might serve to motivate such experiments.

For the dynamically similar $\pi$, $\gamma$ and $\gamma$, $\pi$ reactions on nuclei, the Kroll-Ruderman term $(G_1\vec{\sigma}\cdot\vec{\epsilon}^*)$ in the Blomqvist-Laget[1] operator is generally strongly dominant in determining the cross section. For the $^{15}N(\pi^+,\gamma)^{15}O$(g.s.) reaction, however, there proves to be a very strong dependence on the term in the operator proportional to the pion propagator (the pion-pole term). *This pion-pole term produces a sharp minimum in $\sigma(\theta)$ by destructive interference with the Kroll-Ruderman term.* The sharp destructive interference minimum is sensitive to the pion-pole term; that is, to the electric current of pions in the nuclear medium. Since that current, and the associated pion propagator, could be affected by the enhanced probability of producing virtual pions in the nuclear medium, the location and magnitude of the interference minimum (indeed even observation of its absence) could serve as a measure of meson degrees of freedom. Of course, one would need to very carefully include all other effects, such as pion distortions, isobar propagation, nuclear correlations, etc.; this paper is a step in that direction. At this stage, we believe that the surprising sensitivity to the pion-pole term found for $^{15}N$ offers some encouragement to the idea of using such a reaction to observe the conjectured pion condensation precursors.[2] A second effect pertaining to the Blomqvist-Laget operator involves the $\Delta_{33}$ resonance. At a pion energy of 50 MeV the $\gamma,\pi$ and $\pi,\gamma$ reactions on nuclei generally show little contribution from the $\Delta_{33}$ part of the $(\pi,\gamma)$ or $(\gamma,\pi)$ operator. For $\pi^+,\gamma$ on $^{15}N$, however, the role of the $\Delta_{33}$ is strongly amplified because the $\Delta$ fills in the minimum of $\sigma(\theta)$ near 90°, where the effect is weighted by $\sin\theta$ in forming the total cross section. This feature leads to a substantially increased total cross section near 50 MeV.

The nuclear structure of $^{15}N$(g.s.) and $^{15}O$(g.s.) in first approximation is taken to be a simple one-hole configuration. Many calculations have shown this to be inadequate for such processes as electron scattering.[3] Furthermore, efforts to improve the results by performing major shell model calculations have not yet proved fruitful.[3] In this paper, we compare the $\pi$, $\gamma$ results obtained using the simple one-hole configuration description with those obtained using nuclear wave functions fitted to very recent $M1$ elastic electron scattering[4] and $\beta^+$ decay. The fitted nuclear wave functions yield a decrease in the total $\pi$, $\gamma$ cross section, partic-

ularly near the 50 MeV total cross section peak.

Our procedure is based on earlier $\gamma,\pi$ distorted-wave impulse approximation (DWIA) studies using the Blomqvist-Laget (BL) photoproduction operator.[5] For the $\pi,\gamma$ process we obtain the time reversed form of this BL operator. Most of our calculations have been done at 50 MeV, where the total $\pi,\gamma$ cross section peaks. The location of this peak is shown to be relatively insensitive to the various effects studied.

## II. THE DWIA FOR RADIATIVE CAPTURE

The amplitude for the $\pi,\gamma$ process involves the many-body matrix elements of an operator $\hat{F}$, where the initial and final nuclear states are discrete, and the operator $\hat{F}$ is assumed to be a one-body operator

$$\hat{F}=\sum_{\alpha\beta}\langle\alpha|\hat{f}|\beta\rangle a_\alpha^\dagger a_\beta\ , \tag{1}$$

where $\alpha$ and $\beta$ are single particle quantum numbers (i.e., $\alpha$ denotes $a$, $m$, $m_\tau$, where "$a$" labels the quantum numbers $n_a$, $l_a$, $j_a$). The use of a one-body operator implies neglect of meson exchange and other higher order effects. For radiative capture (RC) of charged pions, no sum over isospin quantum numbers is needed and hence the isospin operator $\tau_+$ can be omitted in specifying the one particle operator $\hat{f}$,

$$\hat{f}_{\rm RC}=\vec{J}^{\,5}_{\rm RC}\cdot\hat{\epsilon}^*_{\vec{k}\lambda}\varphi^{(+)}_{\vec{q}}(r)e^{-i\vec{k}\cdot\vec{r}}\ . \tag{2}$$

The quantity $\vec{J}^{\,5}_{\rm RC}$ is obtained from the Blomqvist-Laget[1] operator for photoproduction by consideration of the time reversal properties of the elementary reaction $\gamma N\rightleftharpoons\pi N$. The method will be detailed in Sec. III. As could be expected, the alterations required by time reversal are manifested as sign changes for some terms of the photoproduction operator, and as incoming to outgoing reversals of boundary conditions and of the associated pion and photon quantum numbers. In Eq. (2) the incoming pion is described by $\varphi^{(+)}_{\vec{q}}$ and the final photon by $\hat{\epsilon}^*_{\vec{k}\lambda}e^{-i\vec{k}\cdot\vec{r}}$.

The Blomqvist-Laget[1] form of the photoproduction operator involves a sum of the standard Born terms (pseudovector $\pi$-$N$ Lagrangian) plus a term which phenomenologically accounts for the $s$-channel formation of a $\Delta_{33}$ resonance. These diagrams are reduced to a nonrelativistic form in a general reference frame. This reduction makes the operator convenient for embedding in a nonrelativistic nuclear calculation since one thereby incorporates the pion-nucleus to pion-nucleon center of mass transformation in a reasonable manner. The operator has as its leading term the Kroll-Ruderman operator, $G_1\vec{\sigma}\cdot\hat{\epsilon}$, which generally dominates photoproduction and radiative capture results at low to moderate energies. There are also "higher order" terms which are generally small relative to the $\vec{\sigma}\cdot\hat{\epsilon}^*$ term, but which for certain reactions may become quite important.

The BL operator is found to give good agreement with experiment for photoproduction of up to 300 MeV pions for the elementary $\gamma N\rightarrow\pi N$ process.[1] This BL description of course also applies, by detailed balance, to the elementary radiative capture process. When used in a nuclear context, however, several approximations are used.[5] The kinematical coefficients of the operators were, for simplicity, evaluated for fixed total nucleon energy ($E_n\sim M_n$). In the elementary reaction this approximation limits the validity of the operator to production of pions below 200 MeV. To embed the operator in a nuclear calculation, one replaces the nucleon and pion momenta, $\vec{p}$ and $\vec{q}$, with the operators $-i\vec{\nabla}_p$ and $-i\nabla_q$.

The overall structure of the nuclear $\pi$, $\gamma$ amplitude[5] is

$$F^{l_\pi m_\pi}_{JM\lambda}=\sum_{LL'}\sum_{n=1}^{12}G_n\int_0^\infty dr\,r^2\rho^{(n)}_{JLL',S}(r)\chi^{(n)l_\pi m_\pi}_{JLL'}(r), \tag{3}$$

from which the cross section is obtained as

$$\sigma(\theta)=\frac{\pi}{2}\frac{2J_f+1}{2J_i+1}\frac{k}{q}\sum_{JM\lambda}\left|\sum_{l_\pi m_\pi}F^{l_\pi m_\pi}_{JM\lambda}Y_{l_\pi m_\pi}(\hat{\theta})\right|^2. \tag{4}$$

The indices $J$, $L'$ and $S$ are, respectively, the total, orbital, and spin angular momentum transferred to the nucleus during the process. This form of the amplitude (3) explicitly demonstrates a separation into a purely nuclear quantity, the transition density $\rho(r)$, where

$$\rho^{(n)}_{JLL',S}(r)=-\sum_{ab}\left(\frac{2j_a+1}{2J+1}\right)^{1/2}\langle\langle a\|\hat{\rho}^{(n)}_{JLL',S}\|b\rangle\rangle \times\langle J_f\|(a_a^\dagger\times\tilde{a}_b)_J\|J_i\rangle\ , \tag{5}$$

and a tensor quantity $\chi(r)$ built from photon multipoles and pion wave functions.[5] The notation $\langle\langle\ \rangle\rangle$ signifies that integrals over nucleon *angular* coordinates have been performed. The quantities $\langle\langle a\|\hat{\rho}^{(n)}_{JLL',S}\|b\rangle\rangle$, for a harmonic oscillator basis, depend only on the nucleon levels and the harmonic oscillator parameter $b'$. The one-body density matrix elements

$$\rho^J_{ab}\equiv\langle J_f\|(a_a^\dagger\times\tilde{a}_b)_J\|J_i\rangle\ , \tag{6}$$

where

$$\tilde{a}_a = (-1)^{j_a - m_a} a_{j_a - m_a}$$

give information on the filling of the shell levels, and hence store the structure information specific to the nuclei involved in the reaction. Evidently, they depend on the initial and final nuclei of the reaction. Thus, given $b'$, only these $\rho^J_{ab}$ are needed to specify the shell model structure of the nuclei. The quantities $\hat{\rho}$ are nucleon operators of the form $[Y_L \times \vec{\sigma}^S]_J$, $[(Y_L \times \vec{\nabla})_{L'} \times \vec{\sigma}^S]_J$, or $[(Y_L \times \vec{\nabla})_{L'} \times \vec{\sigma}^S]_J$ (where $S=0$ or 1 depending on whether the spin matrix is present or not in any particular term in the $\vec{J}^5_{RC}$ operator).

It is, of course, the overlap of the functions $\rho(r)$ and $\chi(r)$ that determines the strength of the transition. The distribution in $r$ of $\rho$ determines those regions of the nucleus most active in the transition. This radial dependence of $\rho$ implicitly tells us where $\chi(r)$ has to be known accurately. Since one part of $\chi(r)$ is the pion distorted wave, the radial dependence of $\chi(r)$ depends directly on the choice of optical potential used for generating $\phi^{(+)}(qr)$. We use an optical potential[5] which fits elastic $\pi$-nucleus scattering at the pion's energy. The computer code PIRK[7] was used to generate the initial pion partial waves. In our calculations, we include all requisite pion partial waves and make corrections for nuclear recoil and the lack of translational invariance of the shell model wave functions.

## III. TIME REVERSAL

To obtain a radiative capture nuclear transition operator as given in Eq. (2), we have time reversed the BL elementary photoproduction (PP) operator.[1] The BL operator $\vec{J}^5$ is characterized by two points. First, each term has an even number of particle momenta. Second, the various terms are differentiated as to whether they contain a Pauli spin matrix or not. The elementary transition matrix element for photoproduction on a nucleon is of the form

$$\langle \chi_f | [\vec{\sigma} S + (\vec{\sigma} \cdot \vec{V}_1)\vec{V}_2 + \vec{V}_3 \times \vec{V}_4] \cdot \hat{\epsilon}_{k\lambda} | \chi_i \rangle , \tag{7}$$

where $S$ and $\vec{V}_1$, $\vec{V}_2$, $\vec{V}_3$, and $\vec{V}_4$ are, respectively, scalar and polar vectors constructed from the pion, photon, and nucleon momenta. By application of the time reversal operator $T$ the above becomes (where $\eta_i, \eta_f$ denote phases)

$$\begin{aligned}\langle T\chi_i | T[\vec{\sigma} S + (\vec{\sigma} \cdot \vec{V}_1)\vec{V}_2 + \vec{V}_3 \times \vec{V}_4] \cdot \hat{\epsilon}_{k\lambda} T^{-1} | T\chi_f \rangle \\ = \eta_i \eta_f \langle \chi^\dagger_{-i} | [-\vec{\sigma} S - (\vec{\sigma} \cdot \vec{V}_1)\vec{V}_2 + \vec{V}_3 \times \vec{V}_4] \cdot \hat{\epsilon}_{k\lambda} | \chi_{-f} \rangle ,\end{aligned} \tag{8}$$

Note that because of the even number of momenta in each term of (7), only the spin dependent terms experience a net sign change under time reversal. Note also that the above result involves no net complex conjugation of either $\hat{\epsilon}_{\vec{k}\lambda}$ or of the operator coefficients. However, $\hat{\epsilon}_{\vec{k}\lambda}$ may be rewritten as $\hat{\epsilon}^*_{-\vec{k}\lambda}$, which describes a final state photon of momentum $-\vec{k}$. Therefore, we have an operator which takes a pion and nucleon of quantum numbers $-\vec{q}$, $-\vec{p}_f$, $-m_f$ to a photon and nucleon of quantum numbers $-\vec{k}$, $-\vec{p}_i$, $-m_i$. Now we consider the physical process with reversed momenta and $m$ quantum numbers ($\vec{q} \to -\vec{q}$, $\vec{k} \to -\vec{k}$, $m_f \to -m_f$, and $m_i \to -m_i$). We are left with an elementary radiative capture operator $\hat{f}_{RC}$ which can be embedded in a nuclear calculation. In that way one obtains the one particle operator

$$\hat{f}_{RC} = \vec{J}^5_{RC} \cdot \hat{\epsilon}^*_{\vec{k}\lambda} e^{-i\vec{k}\cdot\vec{r}} \varphi^{(+)}_{\vec{q}}(\vec{r}) . \tag{9}$$

Recall that the time reversal operator $T = UK_0$ ($K_0$ being complex conjugation and $U$ being unitary); thus

$$\begin{aligned} T_{fi} &= \langle f | \Omega | i \rangle = \langle f | T^\dagger T \Omega T^\dagger T | i \rangle \\ &= K_0 \langle Tf | T\Omega T^\dagger | Ti \rangle = \langle Ti | T\Omega^\dagger T^\dagger | Tf \rangle \\ &= \eta_i \eta_f \langle -i | T\Omega^\dagger T^\dagger | -f \rangle . \end{aligned}$$

The operator $\hat{f}_{RC}$ can also be generated directly from the photoproduction operator,

$$\hat{f}_{PP} = \vec{J}^5_{PP} \cdot \hat{\epsilon}_{\vec{k}\lambda} e^{i\vec{k}\cdot\vec{r}} \varphi^{(-)*}_{\vec{q}}(r) , \tag{10}$$

if one is careful in applying time reversal. The same prescription, Eq. (9), for generating the radiative capture operator, including the correct pion wave function and photon wave function, can be found using

$$\hat{f}_{RC} = T \hat{f}^\dagger_{PP} T^{-1} . \tag{11}$$

Again note that in (11) there is no net complex conjugation of numbers, and that the appropriate time reversed pion and photon wave functions are generated in $\hat{f}_{RC}$ since

$$\begin{aligned} T\varphi^{(-)*\dagger}_{\vec{q}} T^{-1} &= \varphi^{(-)*}_{\vec{q}} = \varphi^{(+)}_{-\vec{q}} , \\ T(\hat{\epsilon}_{\vec{k}\lambda} e^{i\vec{k}\cdot\vec{r}})^\dagger T^{-1} &= \hat{\epsilon}_{\vec{k}\lambda} e^{i\vec{k}\cdot\vec{r}} = \hat{\epsilon}_{-\vec{k}\lambda} e^{i\vec{k}\cdot\vec{r}} . \end{aligned} \tag{12}$$

Thus the time reversal process leads correctly to the reversed pion and photon states: As before, to get $\hat{f}_{RC}$ from (11) we still need to consider the reversed process with $\vec{q} \to -\vec{q}$ and $\vec{k} \to -\vec{k}$. The result (12) for the pion wave function is easily shown for real distorting potentials, but also holds for complex potentials, as a consequence of requiring outgoing waves in $\phi^{(+)}$.[8] The fact that $\phi^{(+)}$ and $\phi^{(-)*}$ satisfy wave equations with the same optical potential ensures that we have

the proper decrease in pion wave flux in both photoproduction and radiative capture. Also the lack of complex conjugation of operator coefficients ensures that the interpretation of the $\Delta_{33}$ contribution remains intact going to radiative capture. The $\Delta_{33}$ contributions are characterized by a complex energy denominator $(W^2 - M_\Delta{}^2 + iM_\Delta\Gamma_\Delta)^{-1}$, where $M_\Delta$ and $\Gamma_\Delta$ are parameters of the resonance and $W$ is the total energy of the pion-nucleon system. If they were to be complex conjugated, the interpretation as a resonance would be destroyed.

This procedure for describing the radiative capture process starting from the $\gamma, \pi$ operators was tested in two ways. The elementary radiative capture operator was deduced in the above time reversal approach and from the basic reversed Feynman diagrams and found to be the same. Secondly, the full configuration space nuclear transition operator was tested via detailed balance by comparing a radiative capture calculation with the appropriately reversed photoproduction calculation. The test was sensitive to the sign changes in each operator. These sign changes are crucial for the conclusion of the paper involving the cross section minimum produced by the pion pole term in the operator.

## IV. RESULTS

In our $\pi, \gamma$ calculations, we have studied the role of nuclear structure, the effects of the optical potential,[10] the $\Delta_{33}$ resonance, and higher order terms in the BL transition operator. The results of each study cannot, of course, be totally separated from those of the others, but clear patterns emerge.

### A. Nuclear structure

The role of nuclear structure was studied by using two sets of wave functions for the $^{15}$N(g.s.)-$^{15}$O(g.s.) system. Since these are mirror nuclei and isospin invariance has been assumed, the wave function for each nucleus in its $J = \frac{1}{2}^-$, $T = \frac{1}{2}$ ground state is essentially the same. Thus one need only specify the wave function of the $^{15}$N nucleus to describe the system. The first set of nuclear wave functions we considered was a simple one-hole configuration. For the $\pi, \gamma$ reaction this configuration gives rise to two nonzero one-body density matrix elements, $\rho^0_{1/2\,1/2}$ and $\rho^1_{1/2\,1/2}$, where $J = 0$, 1 are the two possible transfer angular momenta. The harmonic oscillator parameter $b'$ completes the required nuclear structure information. For the one-hole configuration wave function, $b'$ was taken from elastic electron scattering. A second set of nuclear wave functions was determined by allowing the nonzero $\rho^J_{ab}$ and $b'$ to vary so as to fit both very recent $M1$ electron scattering data[4] and the experimental $ft$ value for $\beta^+$ decay from $^{15}$O(g.s.) to $^{15}$N(g.s.). The $M1$ form factor fitted to the Singhal *et al.* data[4] is compared with the one-hole configuration result in Fig. 1; the corresponding density matrix elements $\rho^J_{ab}$ and value of the oscillator parameter are given in Table I. From Table I, one can see that $\rho^0_{1/2\,1/2}$ is increased in importance relative to $\rho^1_{1/2\,1/2}$, when one fits the recent data.[4] This increase is quite significant in what follows.

Because the transition operator structure in electron scattering is similar to that in our calculation, it is expected that the above fit represents the nuclear structure in a reasonable fashion. To go beyond this fitting procedure would require large scale shell model calculations in the $s$-$d$ shell. While this is certainly feasible, due to the existence of the Glasgow and other codes, it has been shown that the use of the Glasgow code with the standard Kuo interaction yields very little improvement in electron scattering calculations.[3] It is not clear that a proper understanding of this state now exists in terms of a fundamental shell model calculation. Hence we feel that the fitting procedure we adopt is a reasonable approach to

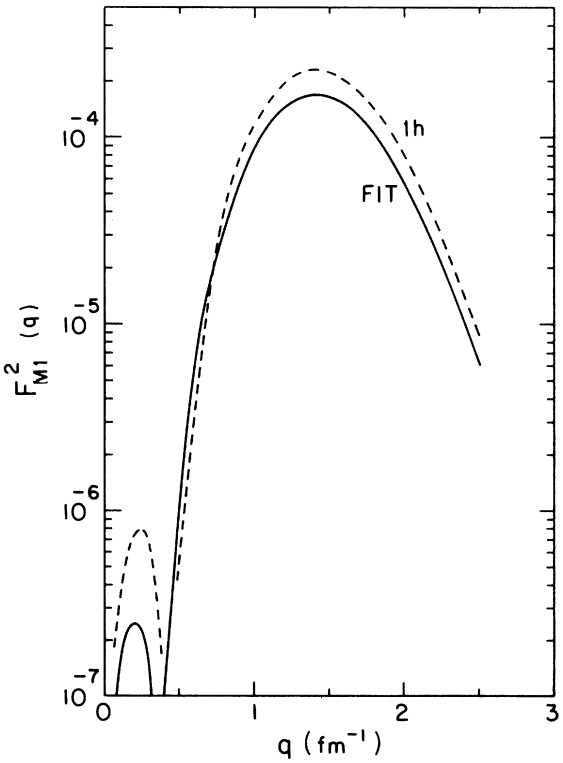


FIG. 1. The $M1$ elastic form factor for $^{15}$N, both for one-hole configuration (---) and for fit to data of Singhal *et al.* (Ref. 4) (——).

TABLE I. One body density matrix elements for $^{15}N(\pi^+,\gamma)^{15}O(g.s.)$ for different nuclear wave functions. The label $J=|\vec{J}_i-\vec{J}_f|=0$, 1 refers to the angular momentum transfer. All other density matrix elements are taken to be zero.

| $\rho^J_{ab}$ | | | one-hole configuration | $M1$ fitted |
|---|---|---|---|---|
| $J$ | $a$ | $b$ | | |
| 0 | $\frac{1}{2}$ | $\frac{1}{2}$ | -0.707 | -0.728 |
| 1 | $\frac{1}{2}$ | $\frac{1}{2}$ | 1.225 | 0.969 |
| $b'$ | (fm) | | 1.74 | 1.68 |

storing the nuclear structure information.

The $\pi,\gamma$ cross section results using fitted wave functions versus those using one-hole wave functions are shown in Figs. 2 and 3. It can be seen from Fig. 2 that the effect on the total cross section of replacing the one-hole nuclear states (dashed curve) by the fitted (solid curve) wave functions is to scale the results down over the 30 to 200 MeV pion energy range. In Fig. 3, we show the corresponding differential cross section $\sigma(\theta)$ calculated for 50 MeV pions. It is seen that $\sigma(\theta)$ is generally lower for the fitted (solid curve) case at all angles except between 30° and 80°. In the 30°–80° range, $\sigma(\theta)$ is not decreased because $\rho^0_{1/2\,1/2}$ is increased in the fitting procedure, and in this angular range the $\pi,\gamma$ operators depending on $\rho^0_{1/2\,1/2}$ prove to dominate. In Fig. 4 the individual contributions of $\rho^0_{1/2\,1/2}$ and $\rho^1_{1/2\,1/2}$ to $\sigma(\theta)$ are displayed (note the $\rho^0$ contribution dominates in the 30°–80° region). Of the operators contributing with $\rho^0_{1/2\,1/2}$ at this energy $\lambda\vec{q}\cdot\hat{\epsilon}^*$ is the strongest by an order of magnitude. The relative importance of $\rho^0_{1/2\,1/2}$ and $\rho^1_{1/2\,1/2}$ changes with angle as shown in Fig. 4; when the $J=0$ and 1 contributions are added the hump at forward angles is generated. Looking at Figs. 5 and 6 one can see, for both plane (Fig. 6) and distorted (Fig. 5) waves, how this hump becomes more pronounced at higher energies. As will be

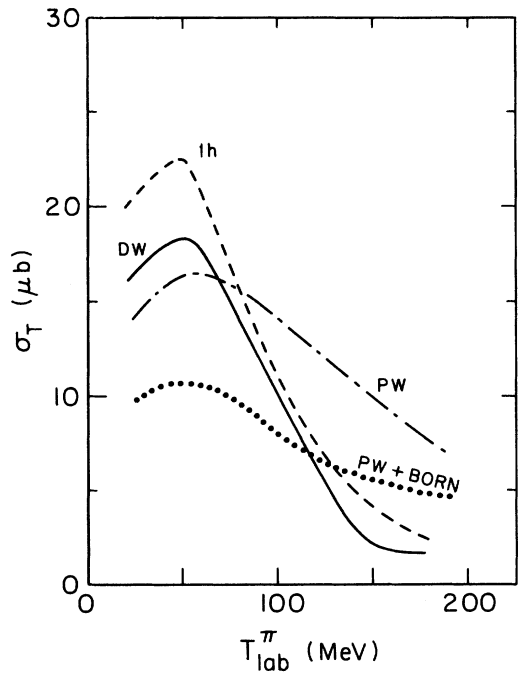


FIG. 2. Radiative capture total cross sections as a function of pion kinetic energy. Full calculation with distorted pion waves, full BL operator, and $M1$ fitted wave functions (——); calculation with distorted waves, full BL operator, and one-hole wave functions (---); calculation with plane waves, full BL operator, and $M1$ fitted wave functions (— - — - —); calculation with plane waves, Born terms only, and $M1$ fitted wave functions (· · ·).

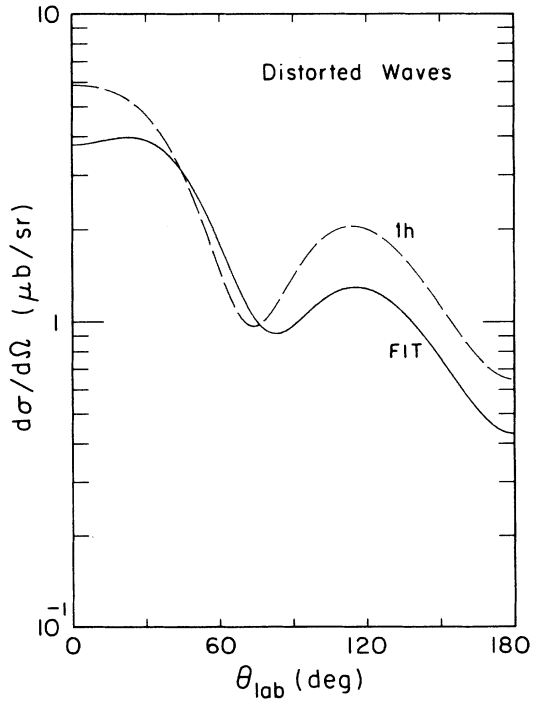


FIG. 3. Differential cross sections for distorted waves and full BL operator at 50 MeV: $\sigma(\theta)$ for $M1$ fitted wave functions (——); $\sigma(\theta)$ for one-hole wave functions (---).

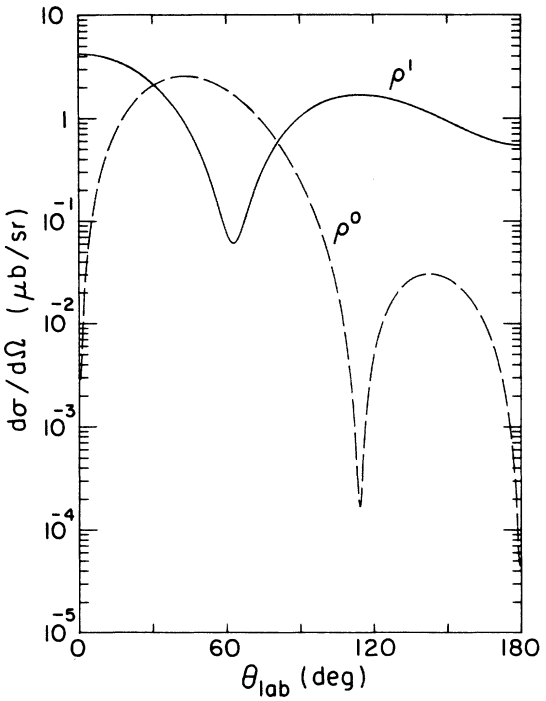


FIG. 4. Individual contributions to $\sigma(\theta)$ of the one body density matrix elements at 50 MeV, calculated with $M1$ fitted wave functions. Contribution of $\rho^1_{1/2\,1/2}$ (——); contribution of $\rho^0_{1/2\,1/2}$ (---). Since the two contributions have different $J$ values, they do not interfere, but add incoherently.

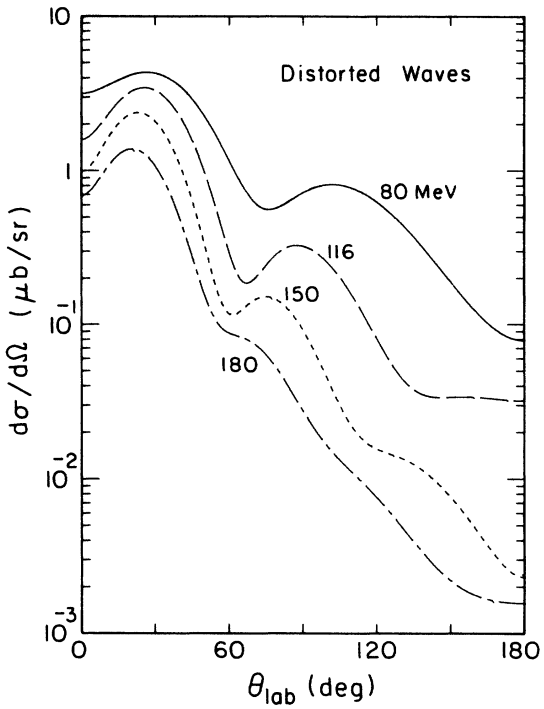


FIG. 5. Differential cross section for distorted waves at increasing pion kinetic energies using $M1$ fitted wave functions and full BL operator: 80 MeV (——); 116 MeV (— — —); 150 MeV (---); 180 MeV (— - — - —).

seen later, this forward angle hump is closely related to the increasing importance of the $\Delta_{33}$ resonance with energy.

One can also see from Fig. 4 that at zero degrees $\sigma(\theta)$ is determined only by $\rho^1_{1/2\,1/2}$ if only two nonzero one-body density matrix elements are assumed. In principle, this fact allows one to measure $\rho^1_{1/2\,1/2}$ directly. This value of $\rho^1_{1/2\,1/2}$ could then be compared both with the one-hole value and that obtainable from fitting electron scattering.

The results of the nuclear structure studies should be viewed with some caution. Our fit to the $M1$ data assumes that only two one-body density matrix elements are adequate to fit the $M1$ form factor data. Actually, we could fit this data only up to 2.5 fm$^{-1}$ with this model. In that range the fit to the data was quite good. However, it is very hard to tell how much nuclear structure information may be stored in this manner.

### B. Optical potential

The optical model potential[6] has quite significant effects on the calculated cross sections as seen

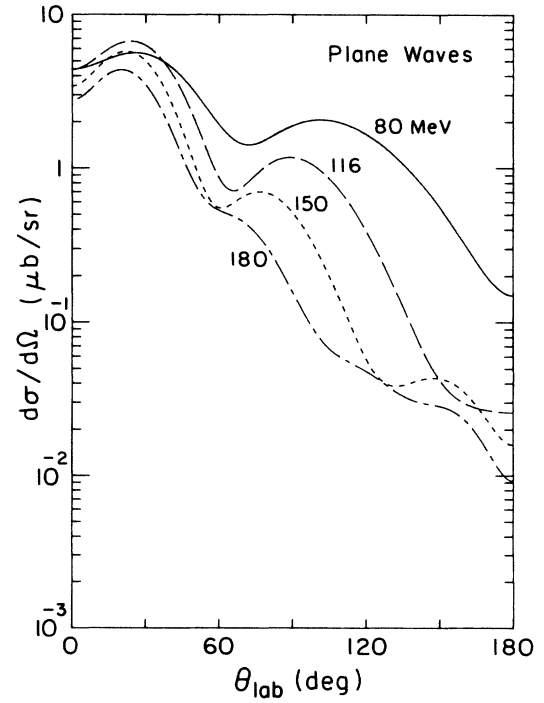


FIG. 6. Differential cross sections for plane waves. Caption same as for Fig. 5.

in Figs. 2 and 7. In Fig. 7 the differential cross sections calculated at 50 MeV for distorted and plane waves are shown. For angles less than about 130°, the cross section is raised by the use of distorted pion waves. For angles greater than this, $\sigma(\theta)$ is lowered. A study was made of how the distorted waves change $\sigma(\theta)$ in the $l_\pi = 0, 1, 2$ partial waves; it was found that the $l_\pi = 2$ wave predominantly accounts for the changes wrought by the distortions. One can see from Fig. 2 that this change in $\sigma(\theta)$ also yields an increase in the total cross section for energies less than about 80 MeV. Beyond this energy, absorption embodied in the optical potential causes the total cross section to die much more rapidly for distorted waves than in the plane wave case (Fig. 2). One can see this effect of the distortions at higher energies manifested in $\sigma(\theta)$ by comparing $\sigma(\theta)$ obtained for plane waves (Fig. 6) and distorted waves (Fig. 5). Whereas the plane wave results for $\sigma(\theta)$ at 0° vary gently, that for distorted waves falls drastically with energy, in agreement with the falloff of the total cross section with energy seen in Fig. 2.

It should be mentioned that the optical potential we have used cannot be tested against $\pi$-$^{15}$N scattering data, as none exists. The Stricker-McManus-Carr (SMC) potential[6] is nominally applicable to all nuclei, but the pion scattering data is essentially limited to even-even nuclei. The SMC potential works well for nuclei near $^{15}$N, but Dytman *et al.*[9] point out that some possibly important valence nucleon effects occur in $\pi$-nucleus scattering. Such valence nucleon effects have not been incorporated for our paper, but should be kept in mind when assessing the effects of the optical potential; we simply adopt the SMC pion optical potential and apply it to $^{15}$N.

### C. $\Delta_{33}$ resonance

The $\Delta_{33}$ resonance has quite marked effects even at the low energies we have studied. As can be seen in Fig. 2 by comparing the total cross section obtained using plane waves and the Born $(\pi, \gamma)$ operator (dotted curve) to the result for plane waves and the full BL $(\pi, \gamma)$ operator (dash-dot curve), one sees that the $\Delta$ resonance terms *of the $\pi, \gamma$ operator* cause the total cross section to increase by ~50% at 50 MeV. The reason for this increase is clear from Fig. 8, which shows $\Delta_{33}$ only, Born only, and Born + $\Delta_{33}$ results for $\sigma(\theta)$. The $\Delta_{33}$ only results, while substantially lower than the Born results at forward and backward angles, peaks just where the sharp dip

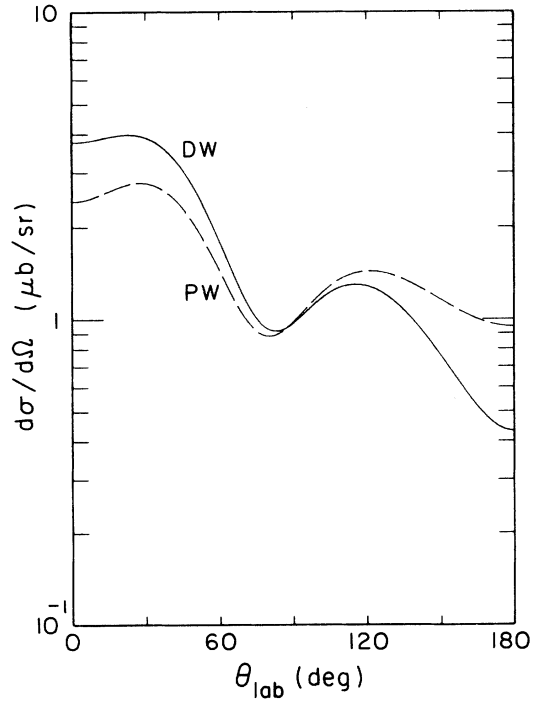


FIG. 7. Differential cross section 50 MeV with distortions, with full BL operator $M1$ fitted wave function. Distorted waves (——); plane waves (— — —).

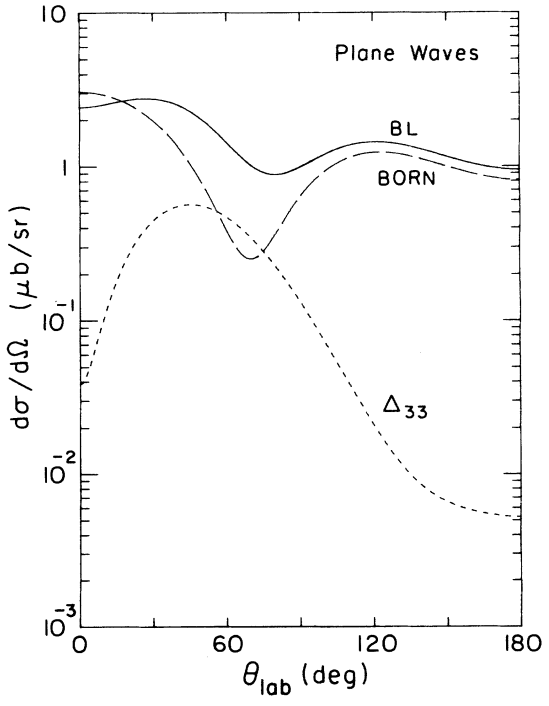


FIG. 8. Differential cross sections at 50 MeV for plane waves and $M1$ fitted wave functions. Full BL operator (——); Born terms only (— — —), and $\Delta_{33}$ terms only (---).

appears in the Born cross section. This serves to fill in the dip and raise the total cross section by the factor shown in Fig. 2.

It was mentioned previously that the $\Delta_{33}$ results and the fact that $\rho^0_{1/2\,1/2}$ gained increased importance relative to $\rho^1_{1/2\,1/2}$ were closely related. This is because at this energy the $\Delta_{33}$ amplitude is dominated by $\lambda\vec{q}\cdot\hat{\epsilon}^*$ (or $\vec{q}\cdot\hat{\epsilon}^*\times\vec{k}$), the same operator which dominates the $\rho^0_{1/2\,1/2}$ results (Fig. 4). For this one operator the $\Delta_{33}$ strength is almost the same as the Born strength. Hence adding in the $\Delta$ term of the $\pi,\gamma$ operator has the same effect as using the fitted wave functions; namely increasing $\sigma(\theta)$ to form the hump seen in Fig. 8. As the energy is raised (see Figs. 5 and 6), one obtains the hump at forward angles whether or not the fitted wave functions are used because of the increased importance of the $\Delta_{33}$. If fitted wave functions are used, the hump is enhanced, but its main origin is in the peaking of the $\Delta_{33}$ contribution shown in Fig. 8.

### D. Pion pole operator

The higher order operator $\lambda\vec{q}\cdot\hat{\epsilon}^*$ has been mentioned several times and its isobar significance stressed. However, the most interesting higher order operator is the pion-pole term. It is more important than $\lambda\vec{q}\cdot\hat{\epsilon}^*$ because it adds coherently (same $J$ value) to the dominant $\sigma\cdot\epsilon^*$ term while $\lambda\vec{q}\cdot\hat{\epsilon}^*$ adds incoherently (different $J$ value). Its presence leads to the dip in the cross section below 90°. As can be seen in Fig. 9 the pion-pole term is dominant near 90°, whereas $\vec{\sigma}\cdot\hat{\epsilon}^*$ dominates at smaller and larger angles. This angle dependence leads to destructive interference and the formation of the dip. When one adds in $\lambda\vec{q}\cdot\hat{\epsilon}^*$ (and the lesser contribution due to the other operators) the dip is filled in substantially, but still remains the dominant feature of $\sigma(\theta)$. As can be seen from Figs. 5 and 6 the appearance of a dip is very little influenced by distortions. It dies out at about the same energy for each case. *Hence we have found that an interesting destructive interference occurs between the pion-pole and the $\vec{\sigma}\cdot\hat{\epsilon}^*$ pion capture contributions.*

The approximations inherent in our model should be kept in mind. The validity of the BL operator is only demonstratable for the elementary reaction. The use of the bare BL operator in a DWIA calculation is possibly dangerous since medium and binding effects are neglected, which conceivably could alter some of our conclusions.

## V. CONCLUSIONS

This study has revealed several interesting features of the $^{15}$N$(\pi^+,\gamma)^{15}$O(g.s.) reaction. It shows

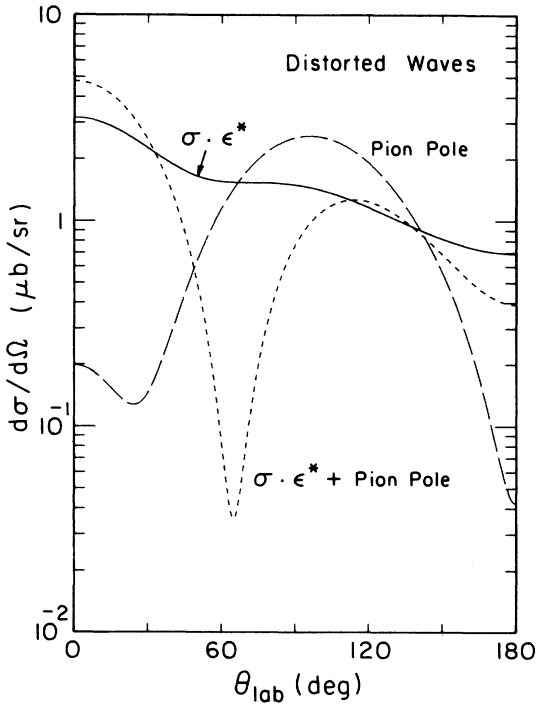


FIG. 9. Differential cross sections with distorted waves and $M1$ fitted wave functions at 50 MeV $\sigma\cdot\epsilon^*$ only (——); pion pole terms only (— — —); $\sigma\cdot\epsilon^*$ plus pion pole terms (---).

strong dependence on some higher order terms in the BL photoproduction operator. Since most calculations involving this operator usually are strongly dominated by the Kroll-Ruderman term, this reaction would be of use in gauging the correctness of these higher order terms. Furthermore, since some of these higher order terms involve the pion derivative, this reaction offers the possibility of testing the pion optical potential.[10] Specific to this reaction is the great importance of the destructive interference generated by the pion pole term in the BL operator. This interference effect has possible implications in the difficult search for pion condensation in finite nuclei.[2] This reaction also shows strong sensitivity to the $\Delta_{33}$ amplitudes in the BL operator. Whereas the $\Delta_{33}$ does not enter so significantly for most photoproduction and radiative capture calculations at 50 MeV, in this reaction, by virtue of the particular nuclear structure information, the $\Delta_{33}$ part of the $\pi,\gamma$ operator greatly enhances the total cross section. For a reaction such as $^{12}$C$(\pi^+,\gamma)^{12}$N in which the $\Delta_{33}$ amplitude essentially follows the $M1$ form factor just as the Born terms do, there is little effect of the $\Delta_{33}$. In the $A=15$ reaction, however, the $\Delta$ amplitude is dominated

by a $J=0$ piece while the amplitude from the $\pi,\gamma$ Born term is dominated by $J=1$. The $\Delta$ contribution peaks where the Born contribution dips and an increase in the total cross section results. Finally the reaction shows strong dependence on the nuclear structure of $^{15}$N and $^{15}$O. Within the context of our model, one can test the 1-hole nature of the wave functions and, in fact, can directly measure the isovector, $J=1$ one-body density matrix element.

*Note added in proof.* Dr. P. Truöl has informed us that radiative capture of in-flight pions are being measured for $A=13$ and 15 nuclear targets at SIN. Also, in a recent report by Delorme *et al.*, this $\pi,\gamma$ reaction has been studied, including pion precursor effects.

## ACKNOWLEDGMENTS

We greatly appreciate the help given by Dr. Mano Singham. We also appreciate the generosity of Dr. R. Singhal who provided us with his very recent elastic $M1$ electron scattering data. We also thank Dr. D. F. Measday whose suggestions prompted our study of the $^{15}$N$(\pi^+,\gamma)^{15}$O(g.s.) reaction. This research was supported in part by the National Science Foundation.

[1] I. Blomqvist and J. M. Laget, Nucl. Phys. A280, 405 (1977).

[2] M. Ericson and J. Delorme, Phys. Lett. 76B, 182 (1978); M. Ericson, in *Mesons in Nuclei*, edited by M. Rho and D. H. Wilkinson (North-Holland, Amsterdam, 1979), Vol. III.

[3] M. W. S. Macauley *et al.*, J. Phys. G 3, 1717 (1977).

[4] R. P. Singhal, R. S. Hick, R. Lindgren, B. Parker, and G. A. Peterson (private communication).

[5] M. K. Singham, G. N. Epstein, and F. Tabakin, Phys. Rev. Lett. 43, 1476 (1979); M. K. Singham and F. Tabakin, Ann. Phys. (N.Y.) (to be published).

[6] K. Stricker, H. McManus, and J. A. Carr, Phys. Rev. C 19, 929 (1979).

[7] R. A. Eisenstein and G. A. Miller, Comput. Phys. Commun. 8, 130 (1974).

[8] N. Austern, in *Direct Nuclear Reaction Theories* (Wiley, New York, 1970).

[9] S. A. Dytman *et al.*, Phys. Rev. C 18, 2317 (1978).

[10] The role of pion distortions in the $\gamma$, $\pi$ reaction has been studied by W. C. Haxton, Phys. Lett. 92B, 37 (1980); B. D. Keister, Phys. Rev. C 18, 1934 (1978); G. N. Epstein, M. K. Singham, and F. Tabakin, *ibid.* 17, 702 (1978). In Ref. 5, the distorted waves were also studied including the higher order gradient terms in the photoproduction operator, which are also included in our present paper for the related $\pi$, $\gamma$ reaction.